Available online at www.sciencedirect.com
SCIENCE DIRECT
Physica A 362 (2006) 151–157
PHYSICA A
www.elsevier.com/locate/physa

# Lattice Boltzmann equation simulation of rectangular jet (AR = 1.5) instability and axis-switching

Huidan Yu*, Sharath S. Girimaji

*Aerospace Engineering Department, Texas A&M University, College Station, TX 77843-3141, USA*

Available online 7 October 2005

**Abstract**

We investigate the axis-switching and instability onset characteristics of a rectangular jet with aspect ratio (AR) of 1.5. Jet flow simulations of four different Reynolds numbers, 10, 100, 150, and 200, are performed. Half-width of streamwise velocity along with velocity vector and streamwise vorticity on transverse planes at different downstream locations are examined. The simulation results show the following instability characteristics: (i) At relatively low Reynolds numbers (10 and 100), the jet flow is laminar and stable; (ii) At $Re = 150$, the flow is still laminar and stable but axis-switching occurs with downstream distance; and (iii) At $Re = 200$, the jet flow becomes unstable but the axis-switching is still seen roughly. Instability first originates near the jet orifice and then propagates down the stream.


*Keywords:* Lattice Boltzmann equation; Rectangular jet; Axis-switching; Instability

## 1. Introduction

Motivated by jet-engine design and flow control needs, extensive investigations of turbulent jet flows have been undertaken experimentally, theoretically, and numerically in the past few decades. Special efforts have been made to study of non-circular jet physics owing to their enhanced entrainment and mixing properties relative to those of comparable circular jets (cf. review [1] and references therein). Rectangular jet (RJ) combines non-unity aspect ratio (AR) feature of elliptic jets with the corner (vertex) feature of square jets. This combination yields features which are of importance in practical applications. Laboratory experiments [2–4] and numerical simulations [5–8] of RJs indicate a peculiar phenomenon called axis-switching. Axis-switching is characterized by the jet cross-section shape axes rotation. As was recognized by many investigators, large-scale coherent structures play a dominant role in the evolution of free mixing layers especially in flows at low Reynolds number (*Re*) [9–11]. Axis-switching is believed to result from faster growth rate of the jet's shear layers along minor axis plane than those along the major axis plane [1]. This also leads to destabilization of the jet flow. However, the underlying fluid dynamical mechanisms of axis-switching and instability onset are far from clear. It is crucial to understand the dynamics and topology of the large-scale coherent structures governing the entrainment and mixing.

*Corresponding author.
*E-mail addresses:* h0y5840@aero.tamu.edu (H. Yu), girimaji@aero.tamu.edu (S.S. Girimaji).

0378-4371/$ - see front matter © 2005 Elsevier B.V. All rights reserved.
doi:10.1016/j.physa.2005.09.035

Lattice Boltzmann equation (LBE) method [12,13] is an attractive numerical tool for direct numerical simulation (DNS) of turbulent flows because of its physical simplicity and computational efficiency [14–16]. Although the single-relaxation-time (SRT) LBE [17,18] based on BGK approximation [19] has been the most popular model in the literature, it has been recently demonstrated that multiple-relaxation-time (MRT) LBE model [20] has better numerical stability [21–23].

In this paper, we study the large-scale flow dynamics of laminar and transitional RJs ($AR = 1.5$) using MRT–LBE. The main objective of this work is to investigate in detail the jet breakdown at relatively low *Re*s at which DNS is feasible. While there have been other experimental and computational studies of RJs, this specific aspect has not been addressed in literature. Therefore, we can only qualitatively assess if our results are consistent with previous studies. Our previous work [8] performs large-eddy simulation (LES) of rectangular turbulent jets at sufficiently high *Re* using MRT–LBE and captured mixing features of rectangular turbulent jet including axis-switching. The computations are in quantitative and qualitative agreements with experimental data. The remainder of this paper is organized as follows. Section 2 briefly formulates the numerical scheme—MRT–LBE. Computation results are presented in Section 3. Finally, we conclude with a brief discussion in Section 4.

## 2. Numerical formulation—Lattice Boltzmann method

We use D3Q19 MRT–LBE model. The formulation details of this model can be found in [21]. Here, we only give a brief introduction. In D3Q19 model, the discrete phase space is defined by a cubic lattice together with a set of discrete velocities $\{\vec{e}_\alpha | \alpha = 0, 1, \ldots, 18\}$. The 19 discrete velocities are $(0,0,0)$ for $\alpha = 0$; $(\pm1,0,0), (0,\pm1,0), (0,0,\pm1)$ for $\alpha = 1-6$, and $(\pm1,\pm1,0), (\pm1,0,\pm1), (0,\pm1,\pm1)$ for $\alpha = 7-18$. A set of velocity distribution functions $\{f_\alpha | \alpha = 0, 1, \ldots, 18\}$ is defined at each node $\vec{x}$ of the lattice. The MRT–LBE is

$$|f(\vec{x} + \vec{e}_\alpha \delta t, t + \delta t)\rangle - |f(\vec{x}, t)\rangle = -M^{-1}\hat{S}[|m(\vec{x}, t)\rangle - |m^{(eq)}(\vec{x}, t)\rangle]. \tag{1}$$

The Dirac notation of ket $|\cdot\rangle$ represents column vector, e.g. $|f\rangle \equiv [f_0, f_1, \ldots, f_{18}]^{\mathrm{T}}$. The collision is executed in a moment space. The moment space $\mathbb{M}$ spanned by the moments $|m\rangle$ and velocity space $\mathbb{V}$ spanned by the distribution functions $|f\rangle$ transfer with each other through a linear mapping $M$: $|m\rangle = M|f\rangle$ or $|f\rangle = M^{-1}|m\rangle$. $\hat{S}$ is the diagonal collision matrix which determines the MRT and $|m^{(eq)}\rangle$ are the corresponding equilibria of $|m\rangle$. The interested macroscopic quantities are obtained by $\rho = \sum_\alpha f_\alpha$ and $\rho\vec{u} = \sum_\alpha \vec{e}_\alpha f_\alpha$.

## 3. Simulations and results

The coordinate system of the simulation field is as follows. The $x$, $y$, and $z$ axes are parallel to streamwise, lateral, and spanwise directions. The whole domain is a $W \times H \times L$ channel. The flow issues with a uniform velocity $u_0$ from a $w \times h$ orifice slot located at the center of the plane ($x = 0$, $-w/2 \leqslant z \leqslant w/2$, and $-h/2 \leqslant y \leqslant h/2$). The *Re* is based on the lateral dimension $h$ of the slot, jet exit velocity $u_0$, and viscosity $v = 151.5e-05$ (cm$^2$/s). The jet orifice is simplified as a plane. We apply bounce-back boundary [24] at jet orifice plane ($x = 0$), fully developed boundary at outflow ($x = L$), and periodic boundary conditions in both spanwise and lateral directions. The parameter details are listed in Table 1. In this work, we focus on the development of the half-width streamwise velocity contour (HWSVC) down the stream at different *Re*s and track the breakdown of the jet due to the flow instability.

Table 1
Details of the simulation cases

| $Re$ | $u_0$ | $w \times h$ | $W \times H \times L$ | Jet exit grid size | Whole domain grid size |
|---|---|---|---|---|---|
| 10 | 1.5 | 1.5,1.0 | 15,10,20 | $12 \times 8$ | $120 \times 80 \times 160$ |
| 100 | 15 | 1.5,1.0 | 11,75,20 | $24 \times 16$ | $180 \times 120 \times 320$ |
| 150 | 22.5 | 1.5,1.0 | 11,75,20 | $24 \times 16$ | $180 \times 120 \times 320$ |
| 200 | 30 | 1.5,1.0 | 11,75,20 | $24 \times 16$ | $180 \times 120 \times 320$ |

Units: length—(cm), time—(s).

The HWSVC evolutions for $Re$s = 10 and 100 are shown in Fig. 1. At these relatively low $Re$s, the flows are laminar and stable. Both jets spread from the initial rectangular shape outwards circles with monotonically increasing radius. Fig. 2 shows the HWSVC evolution at different downstream locations at $Re = 150$. It can

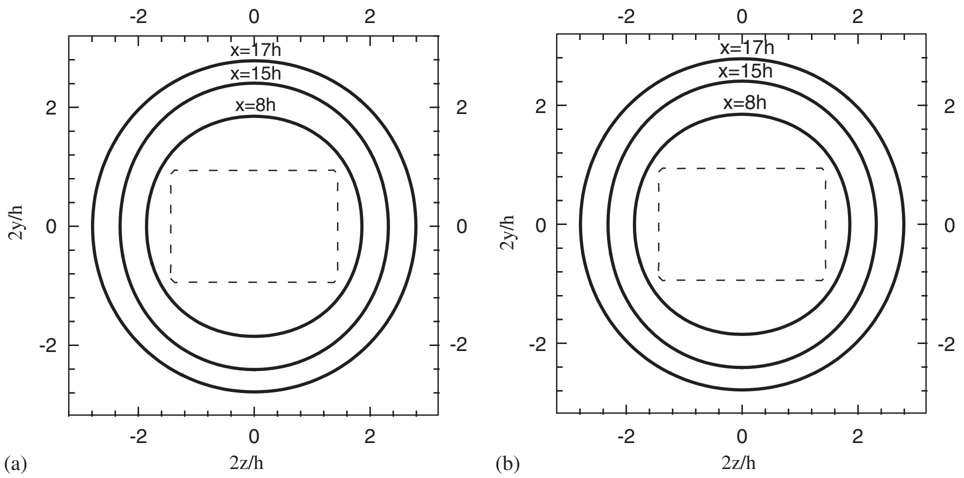


Fig. 1. Half-width streamwise velocity contours at different locations down the stream: (a) $Re = 10$; (b) $Re = 100$. Dashed line is the orifice shape.

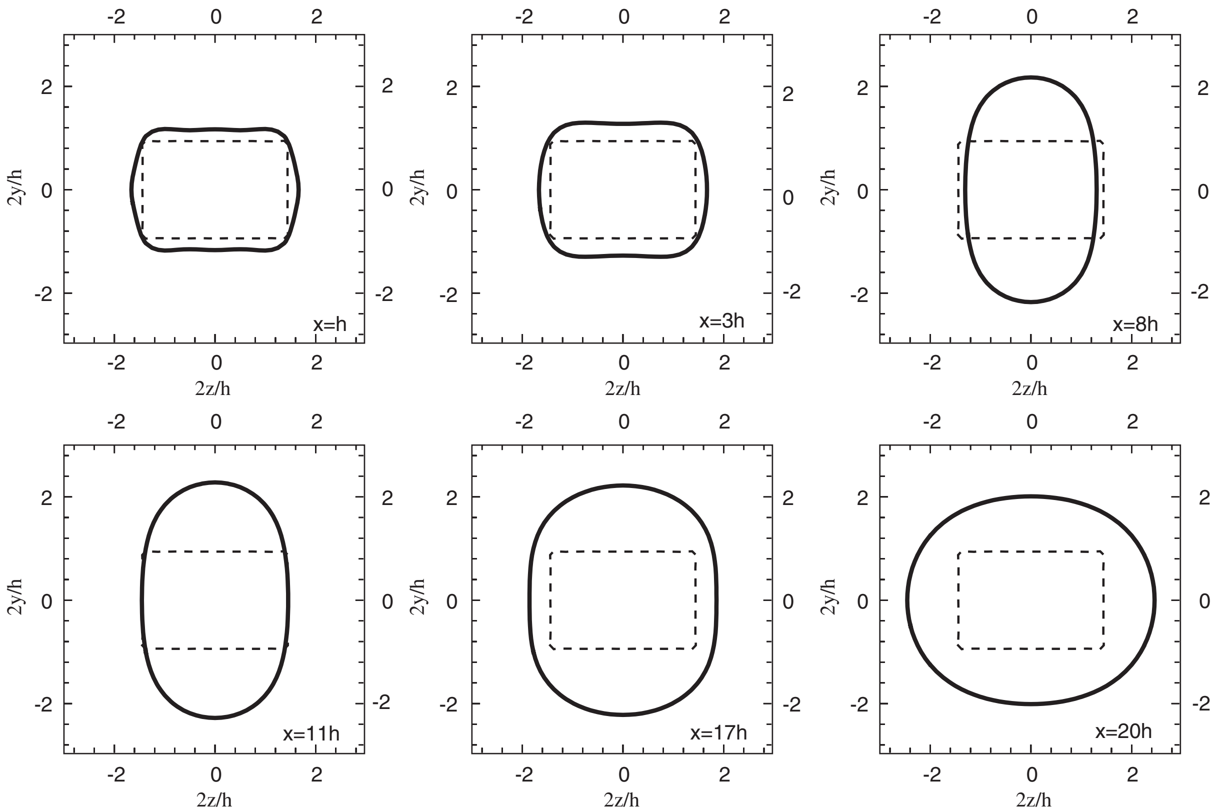


Fig. 2. Half-width contours at $Re = 150$ at different locations down the stream. The jet orifice shape is in dashed line.

be clearly seen that the flow is still laminar and stable but a peculiar phenomenon occurs. The jet spreads from the rectangular shape with the major axis on spanwise direction near the jet orifice (at $x = h$ and $3h$) through an elliptical shape with the major axis on lateral direction in the mediate area (at $x = 8h$, $11h$, and $17h$) to an oval further down the stream (at $x = 20h$) where the major axis returns back to the spanwise direction. This is the pronounced axis-switching behavior. The $Re = 150$ case is particularly interesting as the axis-switching phenomenon can be studied without the complicating influences of transition or turbulence.

Fig. 3 plots the velocity vector fields ($u_y$ and $u_z$) at the same planes as the half-width shown in Fig. 2. At the jet orifice area (at $x = h$ and $x = 3h$), fluid swarms to the center from four directions, stronger along spanwise than lateral direction. Four streams meet and interact near the corners. As a result, flow is stretched along lateral direction slightly. A little further downstream at $x = 8h$ and $11h$, four vortices lead the flow spouting along both sides of lateral direction such that the flow is stretched greatly along the lateral direction, which makes the major axis switch from spanwise to lateral direction. Further downstream, the fluid gushes along spanwise direction at $x = 17h$ and opposite vortices generate at $x = 20h$. The flow is squashed along the lateral direction so that the major axis returns from lateral to spanwise direction.

It is believed that the underlying mechanism of axis-switching behavior results from self-induced Bio-Savart deformation of vortex rings due to non-uniform azimuthal curvature and interaction between azimuthal and streamwise vorticity [1]. From the streamwise vorticity contours at the same planes as in above two plots, see Fig. 4, we can see how axis-switching occurs from a vortex dynamics perspective. At the jet orifice area (at $x = 3h$), vortices are intensive but local. Each quadrant has a pair of vortices both equally strong. At $x = 8h$ where axis-switching occurs, all vortices are still intensive but change the directions. Vortices are still paired in each quadrant but with one strong and one weak. Then the vorticity intensity decreases (at $x = 11h$ and $17h$).

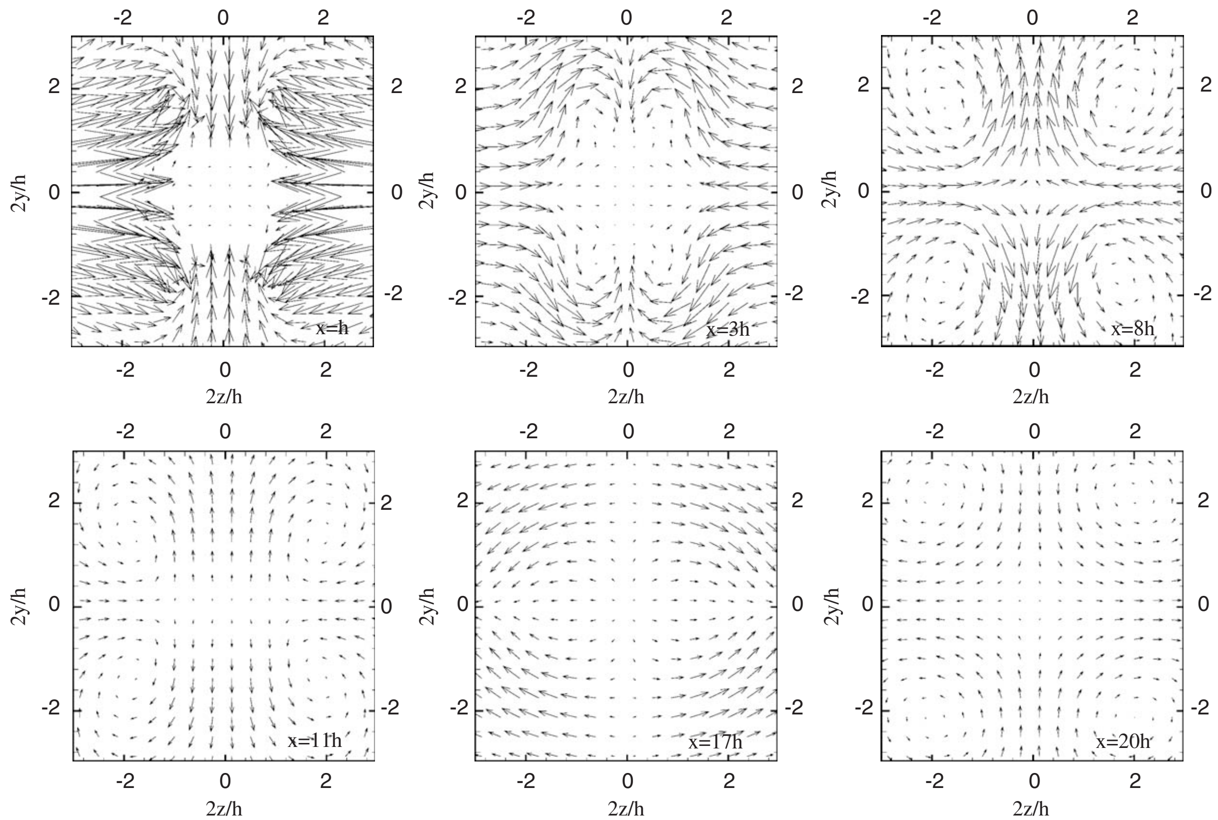


Fig. 3. Velocity vector planes at different downstream locations at $Re = 150$.

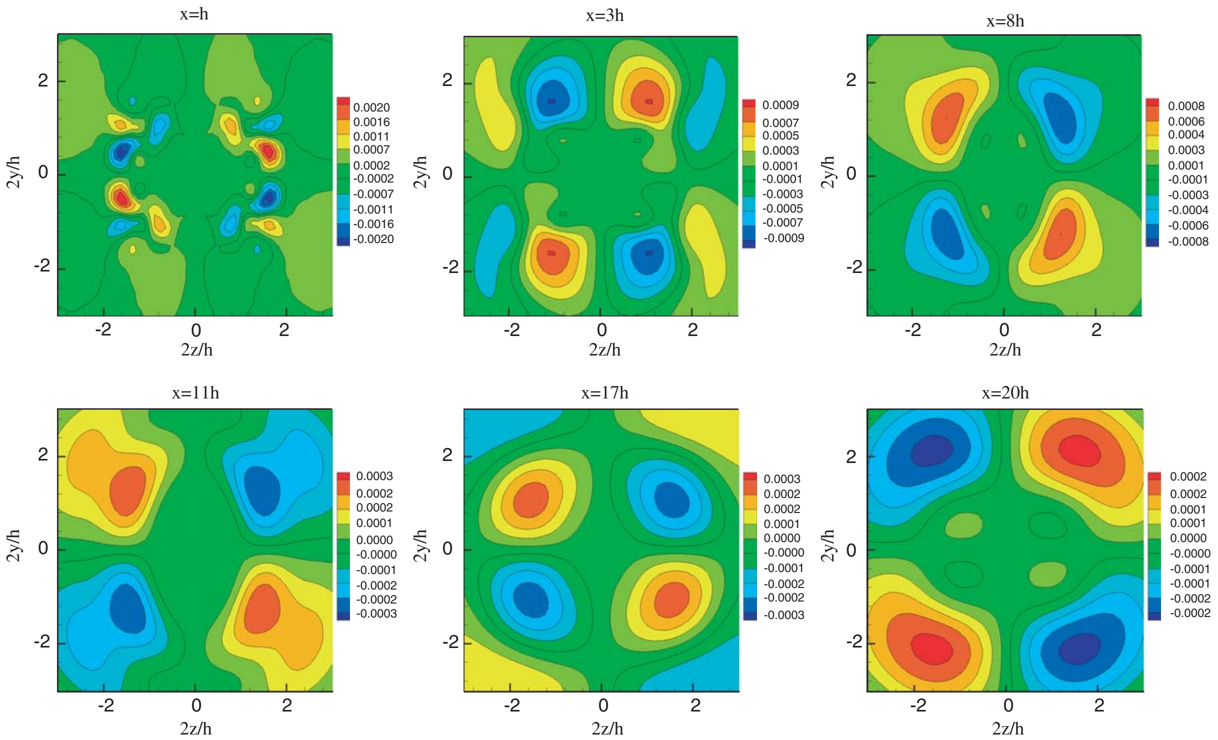


Fig. 4. Streamwise vorticity contour planes at $Re = 150$ on transverse planes at different downstream locations.

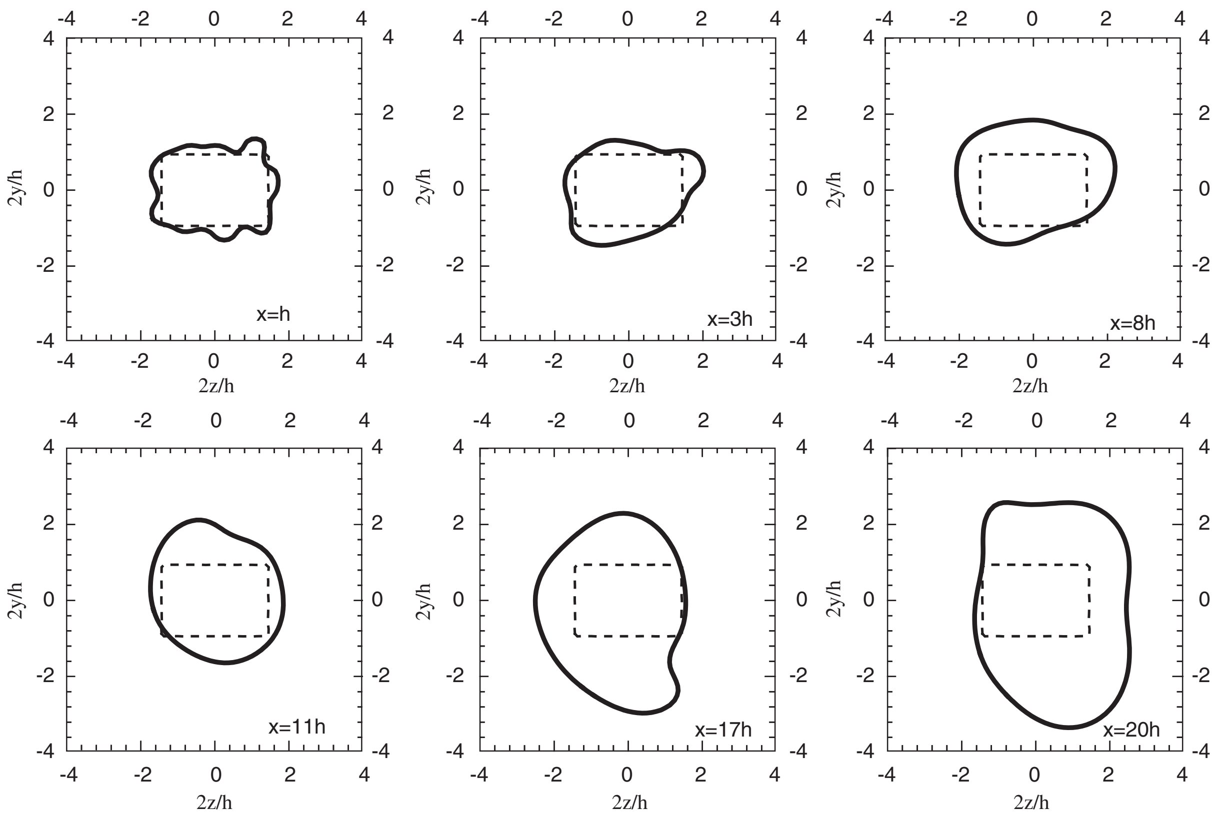


Fig. 5. Late time half-width contour at $Re = 200$ at different locations down the stream. The jet exit shape is in dashed line.

Further down (at $x = 20h$) the vortices change back the direction which brings the major axis back to the spanwise direction.

At higher $Re$ ($= 200$), the jet becomes unstable. At early times, the jet spreads in a similar way to the jet with $Re = 150$ but turns unsteady at later times. It is found that instability first sets in near the jet orifice and then propagates downstream. Fig. 5 shows the evolution of jet HWSVC at a late time. In spite of the instability, the axis-switching is still seen roughly.

## 4. Concluding remarks

We simulate the flow structure of a RJ of $AR = 1.5$. At relatively low $Re$, the jet is laminar and stable. At $Re = 150$, the jet is still laminar and stable but axis-switching occurs. The interactions between spanwise and lateral flow streams clearly show the dynamics of the axis-switching. This phenomenon is also closely related to the vortex dynamics. It is found that jet flow at $Re = 200$ is unstable, even in the absence of density variation and thermal effects. The results of the present simulation are expected to lead to the development of quantitative jet models for axis-switching.

## Acknowledgements

This work was supported by the United States Air Force Office for Scientific Research under Grant No. F49620-01-1-0142.

## References

[1] E.J. Gutmark, F.F. Grinstein, Flow control with noncircular jets, Annu. Rev. Fluid Mech. 31 (1999) 239–272.
[2] Y. Tsuchiya, C. Horikoshi, T. Sato, On the spread of rectangular jets, Exp. Fluids 4 (1986) 197–204.
[3] W.R. Quinn, Turbulent free jet flows issuing from sharp-edged rectangular slots: the influence of slot aspect-ratio, Exp. Therm. Fluid Sci. 5 (1992) 203–215.
[4] W.R. Quinn, Turbulent mixing in a free jet issuing from a low aspect ratio contoured rectangular nozzle, Aeronaut. J. 2110 (1995) 337–342.
[5] B. Rembold, N.A. Adams, L. Kleiser, Direct numerical simulation of a transitional rectangular jet, Int. J. Heat Fluid Flow 23 (2002) 547–553.
[6] R.V. Wilson, A.O. Demuren, Numerical simulation of turbulent jets with rectangular cross-section, J. Fluids Eng. 120 (1998) 285–290.
[7] R.S. Miller, C.K. Madnia, P. Givi, Numerical simulation of non-circular jets, Comput. Fluid 24 (1995) 1–25.
[8] H. Yu, S.S. Girimaji, Near-field turbulent mixing simulations of rectangular jets using lattice Boltzmann method, Phys. Fluid (2005) submitted.
[9] G.L. Brown, A. Roshko, On density effects and large structure in turbulent mixing layers, J. Fluid Mech. 64 (1974) 775–816.
[10] C.M. Ho, L.S. Huang, Subharmonics and vortex merging in mixing layers, J. Fluid Mech. 119 (1982) 443–473.
[11] C.D. Winant, F.K. Browand, Vortex pairing—the mechanism of turbulent mixing layer growth at moderate Reynolds number, J. Fluid Mech. 63 (1974) 237–255.
[12] G. McNamara, G. Zanetti, Use of the Boltzmann equation to simulate lattice-gas automata, Phys. Rev. Lett. 61 (1988) 2332–2335.
[13] F.J. Higuera, J. Jiménez, Boltzmann approach to lattice gas simulations, Europhys. Lett. 9 (1989) 663–668.
[14] S. Chen, G. Doolen, Lattice Boltzmann method for fluid flows, Annu. Rev. Fluid Mech. 30 (1998) 329–364.
[15] L.S. Luo, The lattice-gas and lattice Boltzmann methods: past, present, and future, in: J.H. Wu, Z.J. Zhu (Eds.), International Conference on Applied Computational Fluid Dynamics, Beijing, 2000, pp. 52–83.
[16] D. Yu, R. Mei, L.S. Luo, W. Shyy, Viscous flow computations with the method of lattice Boltzmann equation, Prog. Aerospace Sci. 39 (2003) 329–367.
[17] H. Chen, S. Chen, H.W. Matthaeus, Recovery of the Navier-Stokes equation using a lattice Boltzmann method, Phys. Rev. A 45 (1992) R5339–5342.
[18] Y.H. Qian, D. d'Humières, P. Lallemand, Lattice BGK model for Navier–Stokes equation, Europhys. Lett. 17 (2000) 479–484.
[19] P.L. Bhatnagar, E.P. Gross, M. Krook, A model for collision processes in gases, I. Small amplitude processes in charged and neutral one-component systems, Phys. Rev. 94 (1954) 511–525.
[20] D. d'Humières, Generalized lattice Boltzmann equations, in: B.D. Shizgal, D.P. Weaver (Eds.), Rarefied Gas Dynamics: Theory and Simulations, Prog. Aeronaut. Astronaut, vol. 159, 1992, pp. 450–458.
[21] D. d'Humières, I. Ginzburg, M. Krafczyk, P. Lallemand, L.S. Luo, Multiple-relaxation-time lattice Boltzmann models in three-dimensions, Philo. Trans. R. Soc. London A 360 (2002) 437–451.

[22] P. Lallemand, L.S. Luo, Theory of the lattice Boltzmann method: dispersion, dissipation, isotropy, Galilean invariance and stability, Phys. Rev. E 61 (2000) 6546–6562.
[23] P. Lallemand, L.S. Luo, Theory of the lattice Boltzmann method: Acoustic and thermal properties in two and three dimensions, Phys. Rev. E 68 (2003) 036706-1–25.
[24] L.S. Luo, Theory of the lattice Boltzmann method: lattice Boltzmann models for nonideal gases, Phys. Rev. E 62 (2000) 4982–4996.